Mem. S.A.It. Vol. 94, 233

Memorie della

Integral field spectroscopy allows us to distinguish among the different physical mechanisms affecting galaxies in the different environments

B. Vulcani[1], B. M. Poggianti[1], A. Moretti[1], C. Bacchini[1], S. McGee[2], Y. L. Yaffé[3], M. Mingozzi[4], A. Werle[1], N. Tomičić[5], J. Fritz[6], D. Bettoni[1], A. Wolter[7], and M. Gullieuszik[1]

[1] INAF – Osservatorio Astronomico di Padova, vicolo dell'Osservatorio 5, 35122 Padova, Italy e-mail: `benedetta.vulcani@inaf.it`
[2] University of Birmingham School of Physics and Astronomy, Edgbaston, Birmingham B15 2TT, England
[3] Instituto de Física y Astronomía, Universidad de Valparaíso, Avda. Gran Bretaña 1111 Valparaíso, Chile
[4] Space Telescope Science Institute, 3700 San Martin Drive, Baltimore, MD 21218
[5] INAF- Osservatorio Astronomico di Arcetri, Largo Enrico Fermi 5, I-50125 Firenze, Italy
[6] Instituto de Radioastronomía y Astrofísica, UNAM, Campus Morelia, A.P. 3-72, C.P. 58089, Mexico
[7] INAF- Osservatorio Astronomico di Brera, via Brera 28, I-20121 Milano, Italy

Received: 28-10-2022; Accepted: 22-12-2022

Abstract. Galaxies living in different environments are typically affected by different physical mechanisms. Understanding the frequency of the different processes permits to shed light on galaxy evolution. Spatially resolved maps combined with the knowledge of the hosting environment are a very powerful tool to classify galaxies. The GAs Stripping Phenomena in galaxies (GASP), observed with VLT/MUSE 24 non-cluster galaxies showing asymmetries and disturbances in the optical morphology, suggestive of gas stripping, plus three passive galaxies useful to characterize the final stages of galaxy evolution. We accurately study these galaxies and classify the perturbing mechanisms based on a variety of diagnostics, finding evidence for a wide range of mechanisms. Our analysis shows the successes and limitations of a visual optical selection in pinpointing the processes that influence the gas reservoir of galaxies and probes the power of spatially resolved data in identifying the acting mechanism.

Key words. galaxies: general — galaxies: evolution — galaxies: groups — galaxies: star formation

1. Introduction

Galaxies can inhabit a wide range of environments, from very low (isolated galaxies) to high density (massive cluster cores) regions. In low density environments, galaxies tend to be blue, star-forming and late-type, while dense environments are dominated by red, early-type galaxies. Different physical processes have been invoked to influence the history of galaxies, in most cases leading to a suppression of the star formation. There is no consensus on whether there is one process that dominates quenching across all environments or whether some processes play a larger role in driving galaxy evolution in dense environments than they do in the field (Butcher & Oemler Jr. 1984; Dressler et al. 1999; Poggianti et al. 1999; Treu et al. 2003).

Each of the potential processes that have been proposed is predicted to leave a different signature on the spatial distribution of different components within the galaxy, therefore the study of the spatially resolved properties of galaxies can help understanding the role of the environment on galaxy evolution. While in a few cases processes can feed galaxies with gas, replenishing their fuel for star formation and therefore causing star formation enhancement (Sancisi et al. 2008; Semelin & Combes 2005), most of them typically remove the available gas. For example, ram pressure stripping from the disk due to the interaction between the galaxy interstellar medium (ISM) and the intergalactic medium (IGM; Gunn & Gott 1972) is expected to partially or completely remove the ISM, leaving a truncated Hα disk with smaller extend than the unperturbed stellar disk (e.g., Yagi et al. 2015). Strangulation, which is the removal of the hot gas halo surrounding the galaxy either via ram pressure or via tidal stripping by the halo potential (e.g., Larson et al. 1980; Balogh et al. 2000; Kawata & Mulchaey 2008), should deprive the galaxy of its gas reservoir and leave the existing ISM in the disk to be consumed by star formation. Strong tidal interactions and mergers with other galaxies, and harassment, which is the cumulative effect of several weak and fast tidal encounters (e.g., Toomre & Toomre 1972; Moore et al. 1998), thermal evaporation (Cowie & Songaila 1977), and turbulent/viscous stripping (Nulsen 1982), can also deplete the gas in a an asymmetric way.

The relative influence of these processes depends on several physical parameters that vary from one environment to another. For example, galaxy mergers are rare in clusters because of the large velocity dispersions of the systems and are instead favoured in less dense environments (e.g. Mihos 2004); in contrast, ram pressure stripping is expected to be more effective in the cluster cores because of the large velocities and higher densities of the intracluster medium, while its role in less dense environments is less known.

The Gas Stripping Phenomena in galaxies (GASP[1]) survey is improving our understanding of the processes affecting the gas content of galaxies in different environments, and the environmental conditions that in turn influence the efficiency of these processes. The survey is based on VLT/MUSE observations and therefore delivers maps of many galaxy properties, allowing us to characterize both the ionized gas and the stellar components. GASP explores a wide range of environments, from galaxy clusters to groups and poor groups, filaments and galaxies in isolation. Its targets are located in dark matter halos with masses spanning four orders of magnitude ($10^{11} - 10^{15} M_{\odot}$).

Here we provide a panorama of the different processes taking place in low-density environments and study the reliability of an optical selection in identifying gas removal processes for field galaxies and the power of IFU data in pinning down the acting mechanism.

The cosmological constants assumed are $\Omega_m = 0.3$, $\Omega_\Lambda = 0.7$ and $H_0 = 70$ km s^{-1} Mpc^{-1}.

2. Galaxy Sample and its environment

The GASP program observed with MUSE/VLT 94 galaxies dubbed by Poggianti et al. (2016) “stripping candidates” because they are showing tails, or surrounding debris

[1] http://web.oapd.inaf.it/gasp/index.html

located on one side of the galaxy in their B-band images, plus a sample of 20 undisturbed galaxies.

Here we select all the non cluster stripping candidate galaxies, for a total of 24 galaxies, plus the only 3 morphologically undisturbed ones that are passive.

To define their environment, we make use of three different environmental catalogs: the PM2GC (Calvi et al. 2011), the Tempel et al. (2014) and Saulder et al. (2016) group catalogs. The former extends along an equatorial strip covering an area of ~37.5 $\deg^2$ and is a spectroscopically complete sample of galaxies brighter than $M_B = -18.7$. The latter two are both based on Sloan Digital Sky Survey data. Tempel et al. (2014) is based on SDSS DR10 (York et al. 2000; Ahn et al. 2013), Saulder et al. (2016) used the SDSS DR12 (Alam et al. 2015), combined to the Two Micron All Sky Survey and the 2MASS Redshift Survey (2MASS and 2MRS, Skrutskie et al. 2006; Huchra et al. 2012). However, as a few galaxies do not fall into the SDSS/2MASS footprints and besides the group environment we also need to detect companions that might exert tidal forces, thus we combined MCG (Driver et al. 2005), SDSS, WINGS/OmegaWINGS (Moretti et al. 2014, 2017) and Hyperleda[2] redshifts to get a catalog as complete as possible and downloaded data from the Hyperleda catalog of galaxies with no redshift available, to further detect possible companions.

3. Data analysis

The survey strategy, observations, data reduction and analysis procedure are presented in detail in Poggianti et al. (2017).

Emission line fluxes and errors, along with the underlying continuum, gas velocities (with respect to given redshift), and velocity dispersions were derived using the IDL software KUBEVIZ (Fossati et al. 2016). Stellar kinematics were extracted from the spectra using the Penalized Pixel-Fitting (pPXF) code (Cappellari & Emsellem 2004). Hα luminosities corrected for both stellar absorption and dust extinction were used to compute star formation rates (SFRs), adopting the Kennicutt Jr. (1998)'s relation. The extinction was estimated from the Balmer decrement assuming an intrinsic value Hα/Hβ = 2.86 and the Cardelli et al. (1989) extinction law.

Stellar masses, average SFR and total mass formed in four age bins (= star formation histories, SFH: young = $t < 2 \times 10^7$ yr, recent = $2 \times 10^7 < t < 5.7 \times 10^8$ yr, intermediate-age = $5.7 \times 10^8 < t < 5.7 \times 10^9$ yr, and old => 5.7×10^9 yr); as well as luminosity-weighted stellar ages were derived with the spectrophotometric code SINOPSIS (Fritz et al. 2017).

We employed the standard diagnostic diagrams to separate the regions powered by star formation from regions powered by Active galactic Nuclei (AGN) or Low-Ionization Nuclear Emission Region (LINER) emission (BPT, Baldwin et al. 1981).

Metallicity of the ionized gas was computed for each star-forming spaxel using the pyqz Python v0.8.2 (Dopita et al. 2013) with the MAPPINGS code (see Franchetto et al. 2020, for details).

Structural parameters (effective radius R_e, inclination i, ellipticity ε, position angle PA) were computed on I-band images by measuring the radius of an ellipse including half of the total light of the galaxy (Franchetto et al. 2020).

Integrated values were measured as the sum of all the spaxels within galaxy disks, as defined by (Gullieuszik et al. 2020). Only for metallicity, the integrated value is the mean value computed at the effective radius R_e (Franchetto et al. 2020).

4. Results

A general summary of the global properties of all the 27 galaxies, along with the maps of all useful galaxies properties, can be found in Vulcani et al. (2021). An in depth analysis of 10/27 galaxies can be also found in (Vulcani et al. 2017, 2018a,b, 2019),

To classify galaxies, we mainly inspected the color composite images, the Hα flux maps, the BPT maps, the stellar and gas kinemat-

[2] `http://leda.univ-lyon1.fr`

MECHANISM	Main Environment	Observables
Accretion	Isolation/small group	- **Asymmetric rgb, Hα map** - Regular stellar kinematics - **Asymmetric metallicity map** - Asymmetric mass growth - Counterrotating disk
CWE	Filaments	- **Hα beyond 4 effective radii** - Symmetric stellar kinematics - **Properties of Hα clouds similar to the main body** - **Young Hα cloud**
CWS	Isolation	- **Gas tail** - **Asymmetric gas kinematics** - **Symmetric stellar kinematics** - Evidence for shocks - Stretched metallicity - Young tail
Interaction	One companion	- Asymmetric rgb, Hα map - **Asymmetric stellar and gas kinematics** - **Inhomogeneous stellar velocity dispersione map**
Merger	No clear companion	- **Tidal tail** - Evidence for merger remnants - **Asymmetric stellar and gas kinematics** - **Inhomogeneous stellar velocity dispersion map** - Asymmetric ionized metallicity - Patchy young regions
RPS	Group/cluster	- **Gas tail** - **Asymmetric gas kinematics** - **Symmetric stellar kinematics** - Evidence for shocks - Stretched metallicity - **Young tail** - Central burst
Starvation	?	- No Hα in emission - **Regular stellar kinematics** - **Homogenous SF suppression**

Fig. 1. Summary of the main criteria adopted to pin point the major mechanism acting on galaxies. While the environment is very important for the final classification, not all the observables must occur to safely state the acting mechanism. The critical ones are highlighted in boldface.

ics, the metallicity maps and ages maps (either the luminosity weighted ages or the SFHs in four age bins), and the mass density maps. We then followed the scheme summarized in Fig.1. Thanks to the exquisite quality of the MUSE data, which allows us to study the gas and stellar properties on the kpc scale, we have identified the following mechanisms:

- *Galaxy interactions:* Two galaxies fall in this category. Both of them have a close neighbour, are characterized by a lopsided morphology both in the color composite image and in the Hα map, and have distorted kinematics, in both the stellar and gaseous components. The two cases though are at two stages of interaction: in one case the interacting galaxies are quite similar in mass and size and could be at the first approach, in the other case the companion is much smaller and could have been orbiting around the main galaxy for longer.
- *Mergers:* Seven galaxies enter this category. In one case, also ram pressure signatures are observed. All galaxies show clear tidal tails, and both their stellar and gas kinematics are distorted, evidence of a gravitational interactions. In many cases

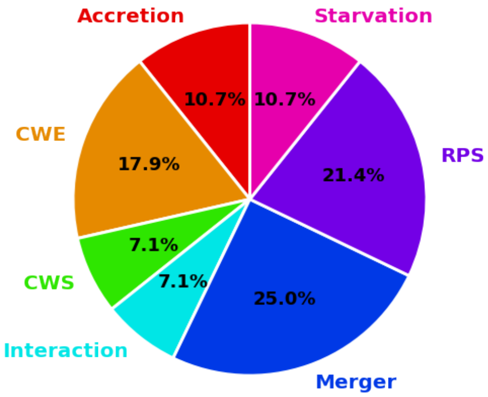

Fig. 2. Pie chart showing the percentage of the different classes in the sample: Accretion (either gas accretion or from a small object), Cosmic web enhancement (CWE), Cosmic web stripping (CWS), Interaction, Merger, Ram pressure stripping (RPS), Starvation.

traces of the merger remnant are visible in the luminosity weighted age and mass maps. Almost all of them have an excess of SFR given their mass, suggesting that new stars were born after the impact. Differences in global properties as sizes and metallicities are most likely due to the diversity in ages, orbits of the mergers and in properties of the progenitors.

– *Ram pressure stripping:* Six galaxies are undergoing ram pressure stripping, one in combination with a merger event. They are all found in groups, massive enough to exert ram pressure on the investigated galaxies. They are clearly at different stages of stripping: one of them has already lost most of its gaseous disk (Vulcani et al. 2018b), is very red and has a low SFR, another one is instead at the peak of its stripping and shows an enhancement of the star formation (especially in the core). In all cases the stellar velocity field is very regular, while the gas kinematics is not. All but the truncated disk show a clear gas tail, and the gas in the tail maintains a coherent rotation with the galaxy, evidence for ongoing stripping. The metallicity gradient in the stellar disk is overall regular, but the metallicity in the tail is lower than at the disk edge. In some cases a bow shock, due to the impact between the galaxy's ISM and ICM, is visible. Finally, the SFH maps point to a recent formation of the tail and shows a strong burst of star formation in the galaxy core during the last $t < 2 \times 10^7$ yr.
– *Cosmic web stripping:* Two galaxies are undergoing this process and are the lowest mass galaxies in the sample, therefore they are in the most favourable position to detect even mild environmental situation. These galaxies have similar properties to the galaxies undergoing ram pressure stripping, but are not located in groups. We therefore hypothesize they feel an interaction with the IGM pervading the cosmic web.
– *Cosmic web enhancement:* Five galaxies belong to this category. They show detached Hα clouds out to large distances from the galaxy center (beyond 4 effective radii). The gas kinematics, metallicity map, and the ratios of emission-line fluxes confirm that they do belong to the galaxy gas disc; the analysis of their spectra shows that very weak stellar continuum is associated with them. Similarly, the SFH and luminosity weighted age maps point to a recent formation of such clouds. Overall, they show an excess of SFR with respect to undisturbed counterparts. All these galaxies are found in filaments, which can foster gas cooling and increase the extent of the star formation in the densest regions in the circumgalactic gas Liao & Gao (2018).
– *Gas accretion:* Three galaxies enter this category. They are characterized by a lopsided morphology, developed only at late times and affecting only the gaseous component, leaving the stellar one mostly unaltered. One of them is most likely undergoing an inflow of low metallicity gas and presents very steep and asymmetric metallicity gradients, while the others are most likely acquiring enriched gas, possibly as a result of a past mergers. In one case, a counter-rotating stellar disk is also observed, indication of gas accretion with an-

gular momentum opposite to that of the host galaxy.
- *Starvation:* The three passive galaxies can be explained invoking starvation, having suppressed SFR homogeneously throughout the disk. The galaxies are redder and have smaller sizes compared to the star-forming population. They are clear examples of passive disks (Bundy et al. 2010).

Figure 2 shows the percentage of galaxies within each class. We remind the reader that GASP targets were selected for showinggalaxies with signs of possible stripping, and galaxies with close companions and with an obvious interaction/merger were avoided as much as possible. Hence, the sample is not suitable for performing general statistics of the most probable processes occurring in the field. It is however interesting to inspect the pie chart to state the 'success' of an optical selection in identifying gas removal processes for field galaxies and probe the power of IFU data in pinning down the acting mechanism.

Overall, the largest group is that of merger, which represents 25% of the full sample, followed by ram pressure stripping (21%) and cosmic web enhancement (18%).

Considering only the star-forming population, hydrodinamical mechanisms, i.e. those that affect only the gas component and leave the stellar properties unaltered (ram pressure stripping, cosmic web enhancement, cosmic web stripping, accretion) affect 65% of the sample, while gravitational interactions are the remaining 35%. Considering that the investigated sample was selected using deep optical imaging to characterize hydrodynamical processes, and great care was taken to exclude merging events and interactions (Poggianti et al. 2016), we can conclude that a visual selection based on optical images can easily mismatch processes affecting both the stellar and gas component and processes that leave the stellar component unaltered. The presence of interacting galaxies also suggests that recognizing companions on the basis of optical images is not trivial, even for expert inspectors.

5. Conclusions

We have analyzed the spatially resolved properties and hosting environment of 24 non-cluster GASP galaxies targeted for showing unilateral debris in the optical imaging (Poggianti et al. 2016) and three non cluster passive galaxies. For each galaxy, we have identified the most probable mechanism.

Galaxies have been classified as follows: 2 galaxy-galaxy interactions, 7 mergers, 4 ram pressure stripped, 2 cosmic web stripped, 5 cosmic web enhanced, 3 undergoing gas accretion, 3 having felt starvation. In one galaxy we identified the combination of merger and ram pressure stripping.

The main conclusion of our analysis is that in non cluster environments a visual inspection of optical images is not reliable to isolate uniquely hydrodynamical processes: almost 2/5 times a visual inspection of B band images is not able to identify processes affecting both the stellar and gas component, nor detect companions, highlighting how difficult it is to identify these processes from optical images. Nevertheless, the information on the hosting environment can be of great help to pinpoint the physical processes affecting galaxies, in particular when combined with spatially-resolved observations.

Acknowledgements. Based on observations collected at the European Organization for Astronomical Research in the Southern Hemisphere under ESO programme 196.B-0578. This project has received funding from the European Research Council (ERC) under the Horizon 2020 research and innovation programme (grant agreement N. 833824). Y.J. acknowledges financial support from ANID BASAL Project FB210003. J.F. acknowledges financial support from the UNAM-DGAPA-PAPIIT IN111620 grant, México.

References

Ahn, C. P., Alexandroff, R., Prieto, C. A., et al. 2013, Astrophysical Journal, Supplement Series, 211, 2014

Alam, S., Albareti, F. D., Prieto, C. A., et al. 2015, Astrophysical Journal, Supplement Series, 219, 12

Baldwin, J. A., Phillips, M. M., & Terlevich, R. 1981, PASP, 93, 5
Balogh, M. L., Navarro, J. F., & Morris, S. L. 2000, Astrophysical Journal, 540, 113
Bundy, K., Scarlata, C., Carollo, C. M., et al. 2010, Astrophysical Journal, 719, 1969
Butcher, H., & Oemler Jr., A. 1984, Astrophysical Journal, 285, 426
Calvi, R., Poggianti, B., & Vulcani, B. 2011, Monthly Notices of the Royal Astronomical Society, 416
Cappellari, M., & Emsellem, E. 2004, Publications of the Astronomical Society of the Pacific, 116, 138
Cardelli, J. A., Clayton, G. C., & Mathis, J. S. 1989, Astrophysical Journal, 345, 245
Cowie, L. L., & Songaila, A. 1977, Nature, 266, 501
Dopita, M. A., Sutherland, R. S., Nicholls, D. C., Kewley, L. J., & Vogt, F. P. A. 2013, Astronomy and Astrophysics Supplement, 208, 10
Dressler, A., Smail, I., Poggianti, B. M., et al. 1999, Astronomy and Astrophysics Supplement, 122, 51
Driver, S. P., Liske, J., Cross, N. J. G., De Propris, R., & Allen, P. D. 2005, Monthly Notices of the Royal Astronomical Society, 360, 81
Fossati, M., Fumagalli, M., Boselli, A., et al. 2016, Monthly Notices of the Royal Astronomical Society, 455, 2028
Franchetto, A., Vulcani, B., Poggianti, B. M., et al. 2020, The Astrophysical Journal, 895, 106
Fritz, J., Moretti, A., Gullieuszik, M., et al. 2017, Astrophysical Journal, 848
Gullieuszik, M., Poggianti, B. M., McGee, S. L., et al. 2020, ApJ, 899, 13
Gunn, J. E., & Gott, J. R. 1972, Astrophysical Journal, 176, 1
Huchra, J. P., MacRi, L. M., Masters, K. L., et al. 2012, The 2MASS Redshift Survey - Description and data release
Kawata, D., & Mulchaey, J. S. 2008, Astrophysical Journal Letters, 672, L103
Kennicutt Jr., R. C. 1998, ARAA, 36, 189
Larson, R. B., Tinsley, B. M., & Caldwell, C. N. 1980, Astrophysical Journal, 237, 692
Liao, S., & Gao, L. 2018, ArXiv e-prints
Mihos, J. C. 2004, Clusters of Galaxies: Probes of Cosmological Structure and Galaxy Evolution, 277
Moore, B., Lake, G., & Katz, N. 1998, Astrophysical Journal, 495, 139
Moretti, A., Poggianti, B., Fasano, G., et al. 2014, Astronomy and Astrophysics, 564
Moretti, A., Gullieuszik, M., Poggianti, B., et al. 2017, Astronomy & Astrophysics, 599, 81
Nulsen, P. E. J. 1982, Monthly Notices of the Royal Astronomical Society, 198, 1007
Poggianti, B., Fasano, G., Omizzolo, A., et al. 2016, Astronomical Journal, 151
Poggianti, B. M., Smail, I., Dressler, A., et al. 1999, Astrophysical Journal, 518, 576
Poggianti, B. M., Moretti, A., Gullieuszik, M., et al. 2017, Astrophysical Journal, 1, 48
Sancisi, R., Fraternali, F., Oosterloo, T., & van der Hulst, T. 2008, Astronomy and Astrophysics Supplement, 15, 189
Saulder, C., Van Kampen, E., Chilingarian, I. V., Mieske, S., & Zeilinger, W. W. 2016, Astronomy and Astrophysics, 596, A14
Semelin, B., & Combes, F. 2005, Astronomy & Astrophysics, 441, 55
Skrutskie, M. F., Cutri, R. M., Stiening, R., et al. 2006, The Astronomical Journal, 131, 1163
Tempel, E., Tamm, A., Gramann, M., et al. 2014, Astronomy & Astrophysics, 566, A1
Toomre, A., & Toomre, J. 1972, Astrophysical Journal, 178, 623
Treu, T., Ellis, R. S., Kneib, J.-P., et al. 2003, Astrophysical Journal, 591, 53
Vulcani, B., Moretti, A., Poggianti, B. B. M., et al. 2017, Astrophysical Journal, 850, 163
Vulcani, B., Poggianti, B., Moretti, A., et al. 2018a, Astrophysical Journal, 852
Vulcani, B., Poggianti, B., Jaffé, Y., et al. 2018b, Monthly Notices of the Royal Astronomical Society, 480
Vulcani, B., Poggianti, B. M., Moretti, A., et al. 2019, Monthly Notices of the Royal Astronomical Society, 487, 2278
—. 2021, The Astrophysical Journal, 914, 27
Yagi, M., Gu, L., Koyama, Y., et al. 2015, The Astrophysical Journal, 149, 36
York, D. G., Adelman, J., Anderson Jr., J. E., et al. 2000, Astronomical Journal, 120, 1579